Journal of Visualized Experiments

A novel right ventricular volume and pressure loaded piglet heart model for the study of tricuspid valve function.

--Manuscript Draft--

Article Type:	Methods Article - JoVE Produced Video
Manuscript Number:	JoVE61251R3
Full Title:	A novel right ventricular volume and pressure loaded piglet heart model for the study of tricuspid valve function.
Section/Category:	JoVE Medicine
Keywords:	Tricuspid valve, porcine heart model, recovery model, thoracotomy, pulmonary valve disruption, pulmonary artery band, echocardiography
Corresponding Author:	Lily Lin University of Alberta Edmonton, Alberta CANADA
Corresponding Author's Institution:	University of Alberta
Corresponding Author E-Mail:	lilylin.pedscardiology@gmail.com
Order of Authors:	Lily Lin
	Sanaz Hatami
	James Yashu Coe
	Timothy M. Colen
	Consolato Sergi
	Richard Thompson
	Elena S. Di Martino
	Walter Herzog
	Ziad Abu Sara
	Darren H. Freed
	Nee Scze Khoo
Additional Information:	
Question	**Response**
Please indicate whether this article will be Standard Access or Open Access.	Standard Access (US$2,400)
Please indicate the **city, state/province, and country** where this article will be **filmed**. Please do not use abbreviations.	Edmonton, Alberta, Canada

Powered by Editorial Manager® and ProduXion Manager® from Aries Systems Corporation

Manuscript Click here to access/download;Manuscript;61251_R3.docx

TITLE:

A Novel Right Ventricular Volume and Pressure Loaded Piglet Heart Model for the Study of Tricuspid Valve Function

AUTHORS AND AFFILIATIONS:

Lily Q. Lin[1], Sanaz Hatami[2], James Yashu Coe[1], Timothy M. Colen[1], Consolato Sergi[3], Richard Thompson[4], Elena S. Di Martino[5], Walter Herzog[6], Ziad Abu Sara[6], Darren H. Freed[2], Nee Scze Khoo[1]

1. Division of Pediatric Cardiology, Department of Pediatrics, University of Alberta, Edmonton, Alberta, Canada
2. Department of Surgery, University of Alberta, Edmonton, Alberta, Canada
3. Department of Laboratory Medicine and Pathology, University of Alberta, Edmonton, Alberta, Canada
4. Department of Biomedical Engineering, University of Alberta, Edmonton, Alberta, Canada
5. Department of Civil Engineering, University of Calgary, Calgary, Alberta, Canada
6. Faculty of Kinesiology, University of Calgary, Calgary, Alberta, Canada

Corresponding author:
Lily Q. Lin
lily.lin@ualberta.ca

Email addresses of Co-authors:
Sanaz Hatami (hatami@ualberta.ca)
James Yashu Coe (jcoe@ualberta.ca)
Timothy M. Colen (colen@ualberta.ca)
Consolato Sergi (sergi@ualberta.ca)
Richard Thompson (richard.thompson@ualberta.ca)
Elena S. Di Martino (edimarti@ucalgary.ca)
Walter Herzog (wherzog@ucalgary.ca)
Ziad Abu Sara (zabusara@ucalgary.ca)
Darren H. Freed (dhfreed@ualberta.ca)
Nee Scze Khoo (khoo@ualberta.ca)

KEYWORDS:

Tricuspid valve, porcine heart model, recovery model, thoracotomy, pulmonary valve disruption, pulmonary artery band, echocardiography

SUMMARY:

A novel recovery piglet heart model with combined pressure and volume overload on the right ventricle is described for the study of tricuspid valve function.

ABSTRACT:

Heart conditions in which the tricuspid valve (TV) faces either increased volume or pressure

stressors are associated with premature valve failure. Mechanistic studies to improve the understanding of the underlying pathophysiology responsible for the development of premature TV failure are lacking. Due to the inability to conduct these studies in humans, an animal model is required. In this manuscript, we describe the protocols for a novel chronic recovery infant piglet heart model for the study of changes in the TV when placed under combined volume and pressure stress. In this model, volume loading of the right ventricular valve and the TV is achieved through the disruption of the pulmonary valve. Then pressure loading is accomplished through the placement of a pulmonary artery band. The success of this model is assessed at four weeks post intervention surgery through echocardiography, intracardiac pressure measurement, and pathologic examination of the heart specimens.

INTRODUCTION:

The normal TV functions in a low volume and pressure stress environment. However, there are pediatric and adult heart conditions where the TV is either congenitally malformed or the cardiac physiology is such that the right ventricle and TV are challenged by increased volume (preload) and/or pressure (afterload) stress, such as Tetralogy of Fallot, Ebstein's anomaly, congenitally corrected transposition of the great arteries, patients with transposition of the great arteries following an atrial switch procedure, idiopathic pulmonary hypertension and hypoplastic left heart syndrome. In these cardiac conditions, the TV is prone to premature valve failure, which increases morbidity and mortality[1–5]. Although one may hypothesize that premature TV failure in these cardiac lesions may be related to the TV being subjected to increased volume and/or pressure stressors, the exact etiology is unknown. Research over the past decade has demonstrated that the mitral valve, the other atrioventricular valve, is capable of eliciting structural changes in response to stressors[6–8]. However, the current literature lacks mechanistic studies that assess TV adaptation to stressors. This aspect may be in part due to a lack of an adequate animal heart model that will allow for such studies.

In the literature, there are models that individually volume or pressure loaded the right ventricle. However, the combination of chronic pressure and volume loading of the right ventricle has been more challenging to achieve. There are animal models in the literature that use placement of a pulmonary artery band to pressure-load the right ventricle as well as creating an atrial septal defect to volume-load the right ventricle[9]. This technique was not able achieve the goal of chronic simultaneous pressure and volume loading of the right ventricle as the presence of tight pulmonary artery bands may result in a right to left shunt across the atrial septal defect. This results in the atrial septal defect no longer providing a volume load to the right ventricle. An atrial septal right to left shunt will result in a cyanotic animal[10]. To overcome this complication, the model requires the exclusion of animals with naturally existing atrial septal defects.

Other models have utilized the hybrid stage I palliation surgery for hypoplastic left heart syndrome in piglets[11]. This is a recovery model that allows for combined pressure and volume loading of the right ventricle. However, the procedure requires expensive balloon-expandable stents that can be financially prohibitive. Studies by Zeltser et al.[12] and Lambert et al.[13] involve cutting through the right ventricular outflow tract and pulmonary valve and then sewing a polytetrafluorethylene patch over top, mimicking the transannular patch Tetralogy of Fallot

repair technique, to volume load the right ventricle. Then pressure loading of the right ventricle is achieved through placement of a pulmonary artery band. This model can be technically challenging and is disadvantaged by leaving a ventriculotomy scar on the right ventricular outflow tract, which may influence RV function and hence TV function.

This study describes an innovative chronic recovery piglet heart model that elicits combined increased pressure and volume stress on the right ventricle without a ventriculotomy. This model will enable mechanistic studies of TV adaptive changes to simultaneous chronic increase in pressure and volume stressors.

PROTOCOL:

The protocol and procedures in this manuscript were developed under the supervision of a veterinarian and performed in compliance with the guidelines of the Canadian Council on Animal Care and the guide for the care and use of laboratory animals. The protocol was approved by the institutional animal care committee at the University of Alberta. All individuals involved in the manuscript procedures received appropriate biosafety training.

1. Pre-procedure preparation, anesthesia and access

1.1. Inclusion criteria: Use both female and male Duroc crossbred piglets between four to five weeks of age for this model. Piglets of this age have a human maturity equivalent to infants between four to six months of age.

1.2. Exclusion criteria: Exclude piglets with patent ductus arteriosus (assessed by echocardiography), cardiac or extracardiac malformation, or where infectious disease was suspected.

1.3. Transfer piglets to the housing facility at least five to seven days prior to surgery for acclimatization.

1.4. A day prior to surgery, examine the piglet to ensure fitness for surgery and absence of signs of illness, such as coughing, emesis, diarrhea, paleness, weakness, lethargy, or skin lesions.

1.5. Fast piglets from solid feed for at least three hours prior to surgery, allowing access to water up to the time of surgery.

1.6. Transfer piglet to the surgical procedure room.

1.7. Administer procedural premedication of atropine (0.04 mg/kg), midazolam (0.2 mg/kg) and ketamine (2 mg/kg) through an intramuscular injection. Also, administer a slow-release preparation of buprenorphine (0.01 mg/kg) subcutaneously for perioperative analgesia.

1.8. On the operating table, place a recirculating water blanket and set the water temperature initially at approximately 40 °C. Adjust the water blanket temperature to maintain core body temperature between 38.0 to 39.5 °C in the piglet.

1.9. Once the jaw is fully relaxed, spray the larynx with 1% lidocaine. Perform standard endotracheal intubation with portable pulse oximeter monitoring.

1.10. Check, attach and ensure proper function of monitoring equipment: pulse oximeter, capnograph, ECG telemetry leads and temperature probe.

1.11. Give the piglet inhaled isoflurane (2-5%) for anesthetic during the surgical procedure, adjusted depending on the depth of anesthesia. Monitor the depth of anesthesia through assessment of heart rate, respiratory rate and breathing pattern, oxygen saturation, eyelid and withdrawal reflex.

1.12. Use the following initial ventilator settings: PEEP of 4 cmH_2O, tidal volume between 8-10 mL/kg and an inspiratory to expiratory ratio of 1:1. The ventilator rate ranges between 26-36/min, adjusted to achieve pCO_2 between 35-42 mmHg on an arterial blood gas analyzed using a point-of-care blood gas analyzer.

1.13. Place the piglet in a supine position. Apply sterile ophthalmic ointment to both eyes for lubrication during procedure.

1.14. Shave hair over the surgical site. Using sterile gauze and disinfectant scrub (povidone-iodine 7.5%), disinfect the chest in a circular movement from inside to outside three times. Wipe away the excess scrub solution with sterile gauze. Using aseptic technique, drape the surgical sites (neck and left side of chest) and surrounding area.

1.15. Using a modified Seldinger technique, place central catheters in both the carotid artery (3.5 French single lumen catheter or 24 gauge IV catheter) and internal jugular vein (five-six French double or triple lumen catheter) for pressure monitoring, blood sampling and venous access during the procedure for medication delivery.

1.16. Administer an intravenous dose of cefazolin (30 mg/kg) for perioperative sepsis prophylaxis and ranitidine (1 mg/kg) for stress ulcer prophylaxis. Initiate intravenous maintenance fluid (D5WNS) through the central venous catheter.

2. Bioptome disruption of pulmonary valve cusps

2.1. After confirmation of surgical plane, perform a left thoracotomy at the third intercostal space to ensure adequate exposure to visualize main pulmonary artery.

2.2. Using sterile gel and a sleeve, perform epicardial echocardiographic study through the left thoracotomy to assess for presence of atrial septal defect, patent ductus arteriosus, and then

sweep through the pulmonary and tricuspid valves to assess for congenital abnormalities.

2.3. Through the left thoracotomy incision, place purse-string sutures on the main pulmonary artery (MPA) and attach to a snare.

2.4. Using a needle introducer, puncture the MPA in the middle of the purse-string sutures and advance a wire. Over the wire, advance a custom-designed flanged seven-French catheter sheath through the MPA incision. Securely anchor the catheter on the surface of the MPA by wrapping purse-string sutures around the catheter flange, and snare can be tightened down (**Figure 1**).

2.5. Introduce a bioptome into the sheath and advance under epicardial echocardiographic guidance to the pulmonary valve.

2.6. Under direct epicardial echocardiographic visualization, use the bioptome to secure bites in the pulmonary valve cusps. Withdraw the bioptome result in cusp tears and disrupt the pulmonary valve.

2.6.1. Repeat this process as needed to achieve moderate to severe pulmonary regurgitation. This is assessed using pulse-wave Doppler interrogation in the branch pulmonary arteries. We aim to achieve a reverse to forward velocity time integral (VTI) ratio between 0.6 to 0.7 at the time of the procedure. Once satisfied, withdraw the bioptome.

2.7. During procedure, administer intravenous infusions of epinephrine (0.05 - 0.15 µg/kg/min) and/or norepinephrine (0.05 - 0.15 µg/kg/min) as required to maintain normal blood pressure during procedure (mean systemic arterial blood pressure between 60 – 80 mmHg).

3. Placement of pulmonary artery band

3.1. Insert a single lumen five-French umbilical catheter through the previously placed sheath and advance it into the right ventricle (RV) for RV pressure monitoring during the placement of a pulmonary artery band.

3.2. Weave either silk or a synthetic, braided non-absorbable suture through the middle of a silastic band for reinforcement and strength. Wrap this silastic band around the MPA in between the pulmonary valve and proximal to the catheter puncture site.

3.3. Through direct RV pressure measurement, tighten the pulmonary artery band and adjust using a vascular clip to achieve ≥60% systemic RV systolic pressure. Once the desired pressure is reached, tie sutures to secure the pulmonary artery band.

3.4. Advance the umbilical catheter across the pulmonary artery band and into the distal MPA for a pull-back pulmonary artery band gradient. Remove the umbilical catheter and sheath.

3.5. Tie off the purse-string suture to close the MPA puncture site (**Figure 2**).

3.6. Close the left thoracotomy incision in three layers using nonabsorbable sutures for the first layer and then absorbable sutures to close the muscle layers. Apply skin staples to close the skin layer.

3.7. Infiltrate around the skin incision with Bupivacaine (0.5%, max dose 2 mg/kg) for local analgesia. Administer a single intravenous dose of meloxicam (0.2 mg/kg) for postoperative analgesia in addition to the previously given subcutaneous slow-release buprenorphine.

3.8. Remove both the arterial and venous central lines and tie off the vessels to ensure hemostasis.

3.9. Apply Hibitane cream (1% chlorhexidine) to the incisions and secure a bandage dressing to cover the incision.

3.10. Turn off inhaled isoflurane. Once piglet is breathing on its own with adequate airway protection mechanisms, extubate with postoperative recovery monitoring and care.

3.11. For prophylaxis of incisional infection, give an empiric five-day course of oral cephalexin 30 mg/kg BID to the piglet.

4. **Echocardiographic assessment**

4.1. Qualitatively assess pulmonary regurgitation by color Doppler and grade from 0 to 4 [0 = none, 1 = trivial (single narrow jet), 2 = mild (single slightly broader jet with jet length < 10 mm, proximal jet width to RV outflow tract ratio < 0.25), 3 = moderate (single or multiple jets with the combined proximal jet width to RV outflow tract ratio between 0.25 to 0.65), and 4 = severe (wide jet with proximal jet width to RV outflow tract ratio > 0.65)].

4.2. In the intervention group, semi-quantify the pulmonary regurgitation by measuring a reverse to forward velocity time integral (VTI) ratio using pulse-wave Doppler in the branch pulmonary artery (**Figure 3**). Grade the severity of tricuspid regurgitation from 0 to 4 through color Doppler assessment [0 = none, 1 = trivial (single narrow jet), 2 = mild (multiple narrow jets), 3 = moderate (wide jet reaching the midportion of the right atrium), and 4 = severe (wide jet reaching the back wall of the right atrium)]. Both the pulmonary and tricuspid valve regurgitation grading systems are in accordance with current guidelines[14–19].

4.3. Assess right ventricular systolic function using right ventricular fractional area change (RV FAC), which was measured by tracing the area bound by endocardial borders of the right ventricle at end-diastole and end-systole in the apical four-chamber view.

4.4. Calculate the RV FAC as the difference between the two areas, expressed as a percentage of the end-diastolic RV area. An RVFAC value < 35% represents abnormal RV systolic function [20].

REPRESENTATIVE RESULTS:

For model validation, ten piglets (5 male and 5 female) that underwent left thoracotomy with pulmonary valve disruption and placement of pulmonary artery band (intervention group, IP) were compared with ten age and gender-match control piglets that underwent left thoracotomy (control group, CP). At baseline, prior to intervention, all the piglets had either none or trivial pulmonary regurgitation with normal right ventricular geometry and function. There was one piglet in the control group with mild tricuspid regurgitation. All remaining piglets had none or trivial tricuspid regurgitation. There was no acute change to tricuspid or pulmonary regurgitation in the control group following thoracotomy. Following intervention, all the piglets in the intervention group had moderate to severe pulmonary regurgitation and tricuspid regurgitation increased from trivial to mild in one piglet. Right ventricular systolic function was normal in both groups. In the intervention group, there was no difference between gender in terms of feasibility or ease of achieving a successful intervention surgery.

Following a four-week recovery period, piglets underwent second anesthesia for direct intracardiac measurement of RV pressure, and epicardial echocardiographic imaging through a sternotomy incision with three-dimensional echocardiographic (3DE) imaging of the tricuspid valve using a matrix X-7 transthoracic transducer on an ultrasound system. This is followed by euthanasia and harvesting of the heart for analysis. Severe pulmonary regurgitation persisted in the intervention group piglets (**Table 1**). On echocardiography, during second anesthesia, the median regurgitant to forward flow VTI ratio was 0.72 (IQR: 0.60, 0.76). The interventional group RV was dilated, as demonstrated by a larger RV end-diastolic area (RVEDA). By direct pressure assessment, the median RV systolic pressure in the intervention group piglets was 78% (IQR: 64.8, 82.5) of systemic pressure. On specimen examination, the intervention piglets had thicker RV free wall and anterior papillary muscle (**Figure 4**, **Table 1**). These indices confirmed the model success in achieving effective chronic pressure and volume loading on the RV. There was worsening of tricuspid valve regurgitation severity and evidence of RV systolic dysfunction in some of the intervention group piglets (**Table 1**).

Tricuspid valve parameters from eight piglet 3DE datasets (four from the intervention group and four from control group) were analyzed using a custom designed MATLAB software[21] as previously described[22]. In brief, end-diastole was defined as the frame after tricuspid valve closure, and end-systole was defined as the frame before tricuspid valve opening. The number of frames between end-diastole and end-systole was counted, and mid-systole was defined as the midpoint. Nine radial planes (separated by 20°) were obtained transecting through the center of the TV annulus (**Figure 5A**), and the annulus was delineated at the leaflet hinge points in mid-systole (**Figure 5B** yellow dot). To delineate the 3D surface of the leaflets, coordinating points were placed along the leaflet from annulus to annulus on each plane (**Figure 5B** red line). All points were converted into spatial coordinates (x, y, and z) and a proprietary software was used to develop 3D models of the TV and it's apparatus for analysis as described in previous publications[15,23]. Briefly, by using the extracted x, y, and z spatial coordinates, the software defined two separate surfaces, one surface that is fit to the TV leaflets and one that is fit to the annulus (**Figure 5C**). The annular bending angle was measured by dividing into anterior and

posterior sections, as defined by the bending points. The annular points in each of these sections were fit with a plane (non-negative least squares), from which the bending angle was measured as the angle between the normal lines for each plane (**Figure 5D**). Our 3DE preliminary findings are that intervention group piglets, when compared with the control group piglets, had tricuspid valve annular dilation, especially in the lateral width dimension. This resulted in a more circular shape annulus. The annular bending angle was preserved. The total tricuspid leaflet area was significantly greater in the intervention group piglets (Table 2). On specimen examination, the tricuspid valve leaflets in the intervention group were subjectively more opaque with thicker chordae tendineae (Figure 6).

The preliminary data supports the model effectiveness in inducing right ventricular changes consistent with chronic pressure and volume overload. In addition, the model was able to demonstrate significant changes to the tricuspid valve geometry as well as tricuspid valve leaflets on gross pathological examination.

Figure 1: **Intraoperative image through the lateral thoracotomy demonstrating the exposure and positioning of the specialized catheter on the main pulmonary artery to allow for bioptome disruption of the pulmonary valve.**

Figure 2: **Intraoperative image after successful pulmonary valve disruption and pulmonary artery band placement.** All of the catheters and sheaths have been removed. The main pulmonary artery puncture site has been sutured closed.

Figure 3: **Echocardiographic image of a pulse-wave Doppler obtained in the branch pulmonary artery.** The antegrade flow is outlined in blue and retrograde flow is outlined in red.

Figure 4: **The right ventricular anterior free wall is exposed through a standard ventriculotomy incision for photography and measurement of wall thickness.** Free wall thickness from sample piglet from the control group (**A**) and intervention group (**B**).

Figure 5: **Analysis of three-dimension echocardiographic datasets of a tricuspid valve.** The dataset is divided by nine transecting planes 20° apart (**A**) with the annulus hinge and leaflet line traced on each sector (**B**). Separate surfaces fitted to the tricuspid valve annulus (yellow) and the leaflets (blue) (**C**) and separate planes fitted to the divided anterior and posterior sections of the tricuspid valve annulus to derive annular bending angle (**D**).

Figure 6: **Tricuspid valves with annulus opened with a cut through the posteroseptal commissure and placed on the imaging stage in a relaxed state exposing the ventricular surface for photography.** Sample tricuspid valve from control (**A**) and intervention group (**B**).

Table 1. **Comparisons of hemodynamic, echocardiographic pathologic parameters between intervention and control piglet groups for model validation.** Data values are expressed as median (25th, 75th percentile) with Mann-Whitney U test p-values reported.

Table 2. **Comparisons of tricuspid valve 3D echocardiographic parameters between intervention and control piglet groups.** Values expressed as median (25th, 75th percentile) with Mann-Whitney test p-values reported.

DISCUSSION:

During the development of this novel heart model, several considerations have impacted the final model design.

Piglet age and surgical exposure

Prior to formulation of the current piglet model, the team has worked on piglet cadavers ranging from one to six weeks of age with the goal to determine the age range where procedural instrumentation and exposure is adequate. As the surgical procedure required direct echocardiographic guidance, the piglet had to be of the appropriate size to allow for an echocardiographic probe to be placed on the epicardium, as well as adequate room to maneuver procedural equipment. From this work, we have determined that a left lateral thoracotomy provided the best exposure to the main pulmonary artery for the procedure. Also, we found that a piglet around 3 to 4-weeks of age was of adequate size for the surgical procedure. In discussion with the research veterinarian and colleagues at the University of Alberta Swine Research and Technology Centre (SRTC) where the piglets were bred, it was determined that a four-week-old piglet had the optimal survival characteristics for the surgical procedure, recovery and interim growth, as this was the earliest age that the piglets were consistently weaned from the sow and fed on their own. The ability to self-feed was essential for successful postoperative care and avoidance of supplemental parental nutrition, which would require additional instrumentation and tubing to remain attached to the piglet postoperatively, posing a potential risk of infection.

In addition, piglets at around four weeks of age have the maturity equivalent to human infants at four to six months of age, thus providing an infant model with rapid growth potential. Furthermore, when we used an older piglet at six-weeks of age, we found that with pulmonary vascular resistance falling, the RV quickly became untrained to handle the acute increase in pressure applied by the pulmonary artery band. Six-week-old piglets were more hemodynamically unstable to slight changes in pulmonary artery band tightness, and we were only able to achieve approximately half systemic RV systolic pressure. Any further tightening of the pulmonary artery band resulted in acute RV failure and low cardiac output.

Fasting and perioperative analgesia

We routinely fast the piglets from their creep feed approximately three hours prior to surgery. We have found that extended fasting periods at this age was associated with perioperative hypoglycemia. As the surgical field is above the diaphragm, we have not encountered significant concerns with aspiration, postoperative emesis or ileus.

For perioperative analgesia, we used a specially compounded slow-release buprenorphine that was effective over 72 hours. Regular buprenorphine would require an intramuscular or intravenous injection once every three to four hours. We found that administering the slow-release formulation of buprenorphine dramatically improved our postoperative analgesia. The

addition of scheduled oral doses of meloxicam (0.2-0.3mg/kg daily) and acetaminophen (15mg/kg BID-TID) for break-through pain provided excellent perioperative analgesia.

Circulatory support during the procedure

During the pulmonary valve disruption and placement of pulmonary artery band, periods of hypotension may occur with cardiac manipulation. A combination of epinephrine (0.05-0.15 µg/kg/min) and norepinephrine (0.05-0.15 µg/kg/min) infusion was used to maintain blood pressure. Prior to pulmonary valve disruption, it is important to ensure blood pressure is within the normal range, as the acute volume loading due to pulmonary regurgitation can be poorly tolerated. Furthermore, we have found by maintaining blood pressure in high normal range (systolic blood pressure 80 – 90 mmHg, mean arterial pressure 70 – 80 mmHg) allowed for better tolerance of pulmonary artery band placement.

Frequent non-sustained atrial and ventricular ectopy occurred during cardiac manipulation. These ectopies may progress to atrial or ventricular tachycardia; hence, it is important to have defibrillator paddles available on-site to treat unstable tachyarrhythmias.

Morbidity and mortality in follow-up

During model development, we had one piglet die an hour following intervention procedure due to hemorrhage from a right ventricular outflow tract laceration that was not identified at the time of the procedure. The laceration was secondary to using a long and stiff bioptome. We also had one piglet in the intervention group that developed an infectious pericarditis late and died in the second postoperative week secondary to pericardial effusion with tamponade.

Over the follow-up period, the most common morbidity encountered was a localized superficial wound infection at the thoracotomy incision site. This occurred in approximately 40% of the animals. Fortunately, all animals were successfully treated with a ten-day course of oral cephalexin. In the third week following procedure, a few piglets in the intervention group developed mild heart failure symptoms manifested as increased respiratory rate and work of breathing following play activity. The heart failure symptoms were improved with once or twice daily 10 mg of furosemide.

We describe a novel piglet model that enables combined chronic pressure and volume load on the right ventricle through disruption of the pulmonary valve and placement of a pulmonary artery band. Common challenges encountered during the procedure and follow-up is described with suggestions for troubleshooting. This piglet model will enable studies to assess the impact of combined volume and pressure loading on the right ventricle and tricuspid valve.

ACKNOWLEDGMENTS:

This research work was supported through generous grant funding provided by the Stollery Children's Hospital Foundation through the Women and Children's Hospital Research Institute.

DISCLOSURES:

The authors have no disclosures.

REFERENCES:

1. Bokma, J.P. et al. Severe tricuspid regurgitation is predictive for adverse events in tetralogy of Fallot. *Heart*. **101** (10), 794–799 (2015).
2. Wertaschnigg, D. et al. Contemporary Outcomes and Factors Associated With Mortality After a Fetal or Neonatal Diagnosis of Ebstein Anomaly and Tricuspid Valve Disease. *Canadian Journal of Cardiology*. **32** (12), 1500–1506 (2016).
3. De León, L.E. et al. Mid-Term Outcomes in Patients with Congenitally Corrected Transposition of the Great Arteries: A Single Center Experience. *Journal of the American College of Surgeons*. **224** (4), 707–715 (2017).
4. Agnetti, A. et al. Long-term outcome after senning operation for transposition of the great arteries. *Clinical Cardiology*. **27** (11), 611–614 (2004).
5. Chen, L. et al. The prognostic significance of tricuspid valve regurgitation in pulmonary arterial hypertension. *Clinical Respiratory Journal*. **12** (4), 1572–1580 (2018).
6. Dal-Bianco, J.P. et al. Active adaptation of the tethered mitral valve: Insights into a compensatory mechanism for functional mitral regurgitation. *Circulation*. **120** (4), 334–342 (2009).
7. Chaput, M. et al. Mitral leaflet adaptation to ventricular remodeling occurrence and adequacy in patients with functional mitral regurgitation. *Circulation*. **118** (8), 845–852 (2008).
8. Rausch, M.K., Tibayan, F.A., Craig Miller, D., Kuhl, E. Evidence of adaptive mitral leaflet growth. *Journal of the Mechanical Behavior of Biomedical Materials*. **15**, 208–217 (2012).
9. Marino, T.A., Kent, R.L., Uboh, C.E. Structural analysis of pressure versus volume overload hypertrophy of cat right ventricle. *American Journal of Physiology - Heart and Circulatory Physiology*. **18** (2) (1985).
10. Xu, Y., Liu, Y., Lv, X., Yu, C., Li, X. A Novel Hybrid Method for Creating a Porcine Model of Cyanotic Congenital Heart Defect With Decreased Pulmonary Blood Flow. *Journal of Surgical Research*. **154** (2), 262–266 (2009).
11. Holzer, R.J. et al. An animal model for hybrid stage i palliation of hypoplastic left heart syndrome. *Pediatric Cardiology*. **30** (7), 922–927 (2009).
12. Zeltser, I. et al. The roles of chronic pressure and volume overload states in induction of arrhythmias: An animal model of physiologic sequelae after repair of tetralogy of Fallot. *Journal of Thoracic and Cardiovascular Surgery*. **130** (6), 1542–1548 (2005).
13. Lambert, V. et al. Right ventricular failure secondary to chronic overload in congenital heart disease: An experimental model for therapeutic innovation. *Journal of Thoracic and Cardiovascular Surgery*. **139** (5) (2010).
14. Nii, M., Guerra, V., Roman, K.S., Macgowan, C.K., Smallhorn, J.F. Three-dimensional Tricuspid Annular Function Provides Insight into the Mechanisms of Tricuspid Valve Regurgitation in Classic Hypoplastic Left Heart Syndrome. *Journal of the American Society of Echocardiography*. **19** (4), 391–402 (2006).
15. Takahashi, K. et al. Real-time 3-dimensional echocardiography provides new insight into mechanisms of tricuspid valve regurgitation in patients with hypoplastic left heart syndrome. *Circulation*. **120** (12), 1091–1098 (2009).
16. Kutty, S. et al. Tricuspid regurgitation in hypoplastic left heart syndrome mechanistic insights from 3-dimensional echocardiography and relationship with outcomes. *Circulation:*

Cardiovascular Imaging. **7** (5), 765–772 (2014).
17. Lin, L.Q. et al. Reduced Right Ventricular Fractional Area Change, Strain, and Strain Rate before Bidirectional Cavopulmonary Anastomosis is Associated with Medium-Term Mortality for Children with Hypoplastic Left Heart Syndrome. *Journal of the American Society of Echocardiography*. **31** (7), 831–842 (2018).
18. Lancellotti, P. et al. European Association of Echocardiography recommendations for the assessment of valvular regurgitation. Part 1: Aortic and pulmonary regurgitation (native valve disease). *European Journal of Echocardiography*. **11** (3), 223–244 (2010).
19. Zoghbi, W.A. et al. Recommendations for Noninvasive Evaluation of Native Valvular Regurgitation: A Report from the American Society of Echocardiography Developed in Collaboration with the Society for Cardiovascular Magnetic Resonance. *Journal of the American Society of Echocardiography*. **30** (4), 303–371 (2017).
20. Rudski, L.G. et al. Guidelines for the Echocardiographic Assessment of the Right Heart in Adults: A Report from the American Society of Echocardiography. Endorsed by the European Association of Echocardiography, a registered branch of the European Society of Cardiology, and. *Journal of the American Society of Echocardiography*. **23** (7), 685–713 (2010).
21. MATLAB, 2015. Version 8.5.0.197613 (R2015a). Natick, Massachusetts: The MathWorks Inc.
22. Colen, T. et al. Tricuspid Valve Adaptation during the First Interstage Period in Hypoplastic Left Heart Syndrome. *Journal of the American Society of Echocardiography*. **31**, 624–33 (2018).
23. Takahashi, K. et al. Quantitative real-time three-dimensional echocardiography provides new insight into the mechanisms of mitral valve regurgitation post-repair of atrioventricular septal defect. *Journal of the American Society of Echocardiography*. **25** (11), 1231–1244 (2012).

Intraoperative image through the lateral thoracotomy demonstrating the exposure and positioning of the specialized catheter on the main pulmonary artery to allow for

Click here to access/download;Figure;Figure 1.jpg

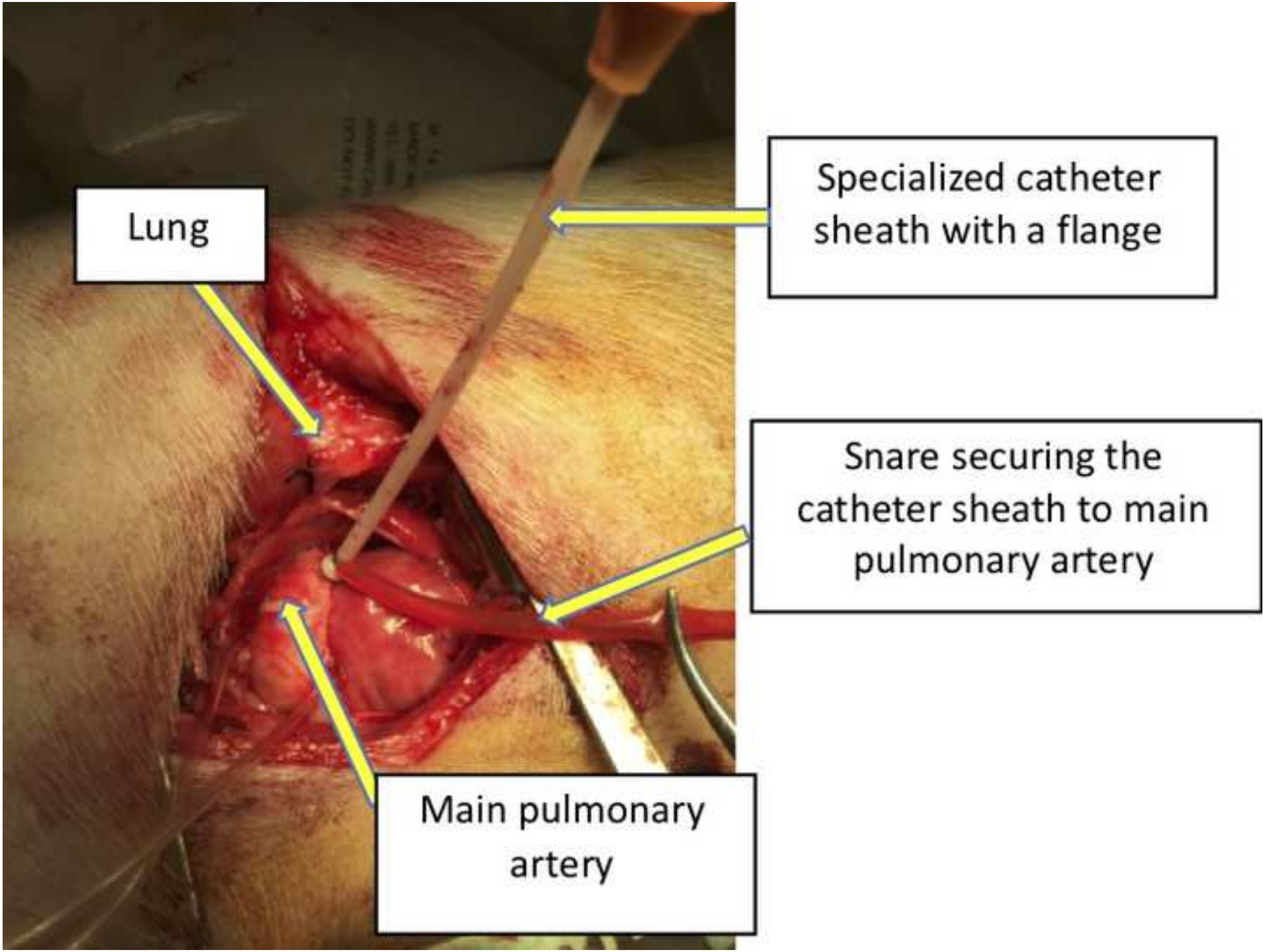

Intraoperative image after successful pulmonary valve disruption and pulmonary artery band placement. All of the catheters and sheaths have been removed. The main

Click here to access/download;Figure;Figure 2.jpg

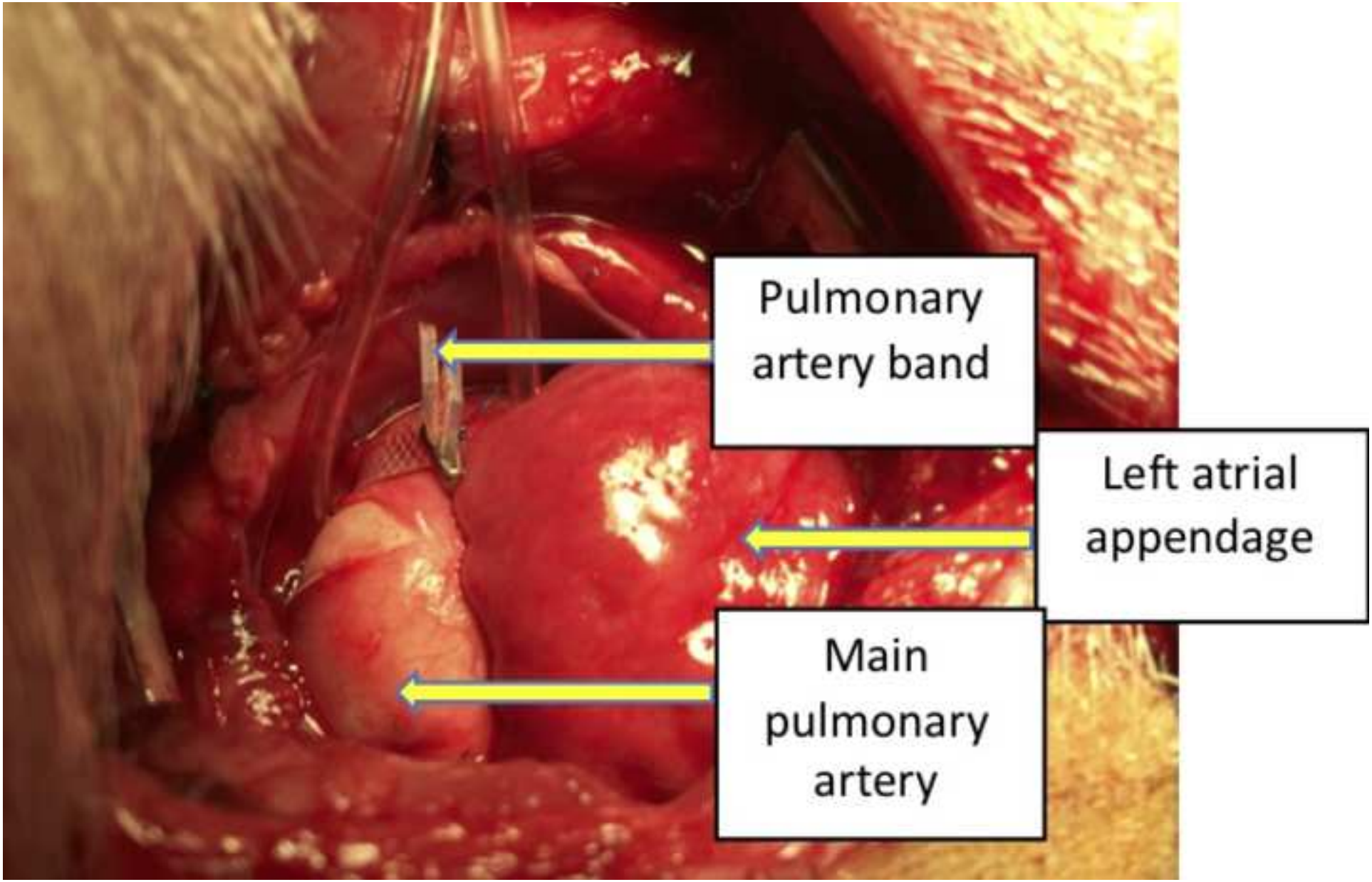

Echocardiographic image of a pulse-wave Doppler obtained in the branch pulmonary artery. The antegrade flow is outlined in blue and retrograde flow is outlined in red.

Click here to access/download;Figure;Figure 3.jpg

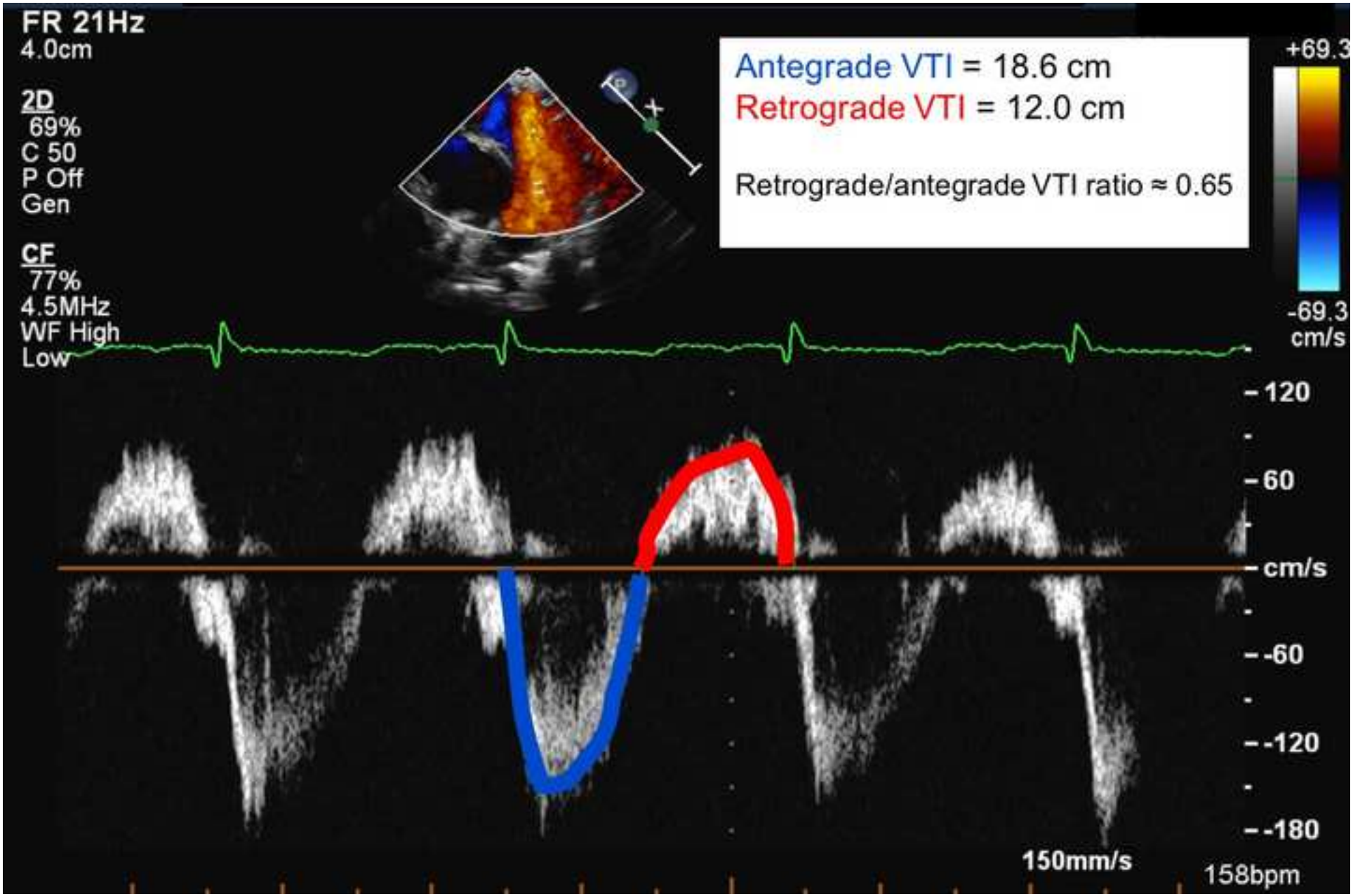

The right ventricular anterior free wall is exposed through a standard ventriculotomy incision for photography and measurement of wall thickness. Free wall thickness from

Click here to access/download;Figure;Figure 4.jpg

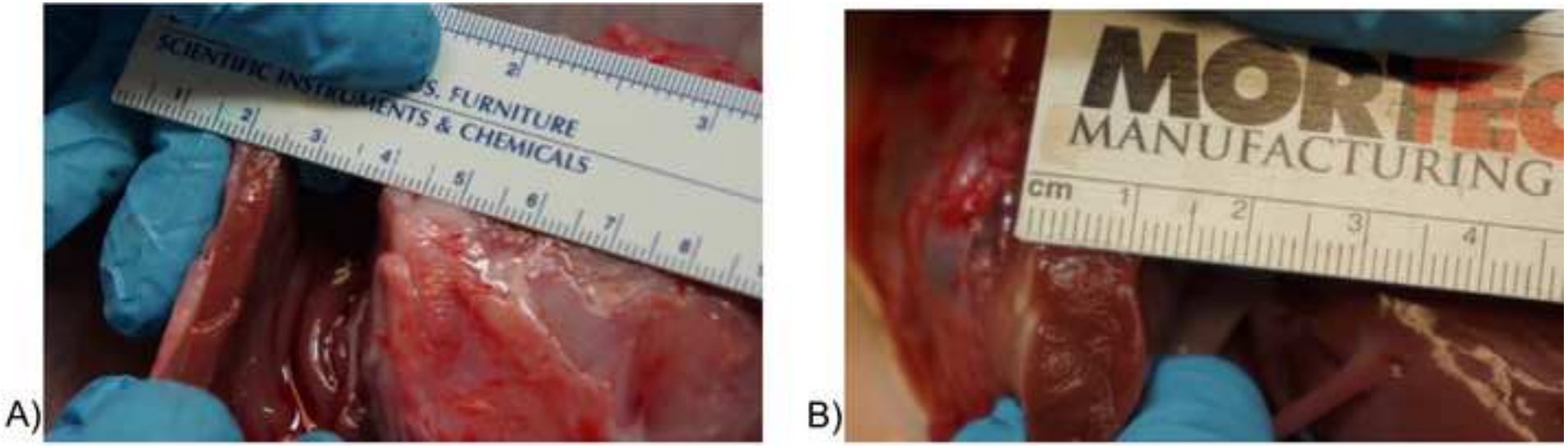

Analysis of three-dimension echocardiographic datasets of a tricuspid valve. Please see figure legend file as unable to upload full description.

Click here to access/download;Figure;Figure 5.jpg

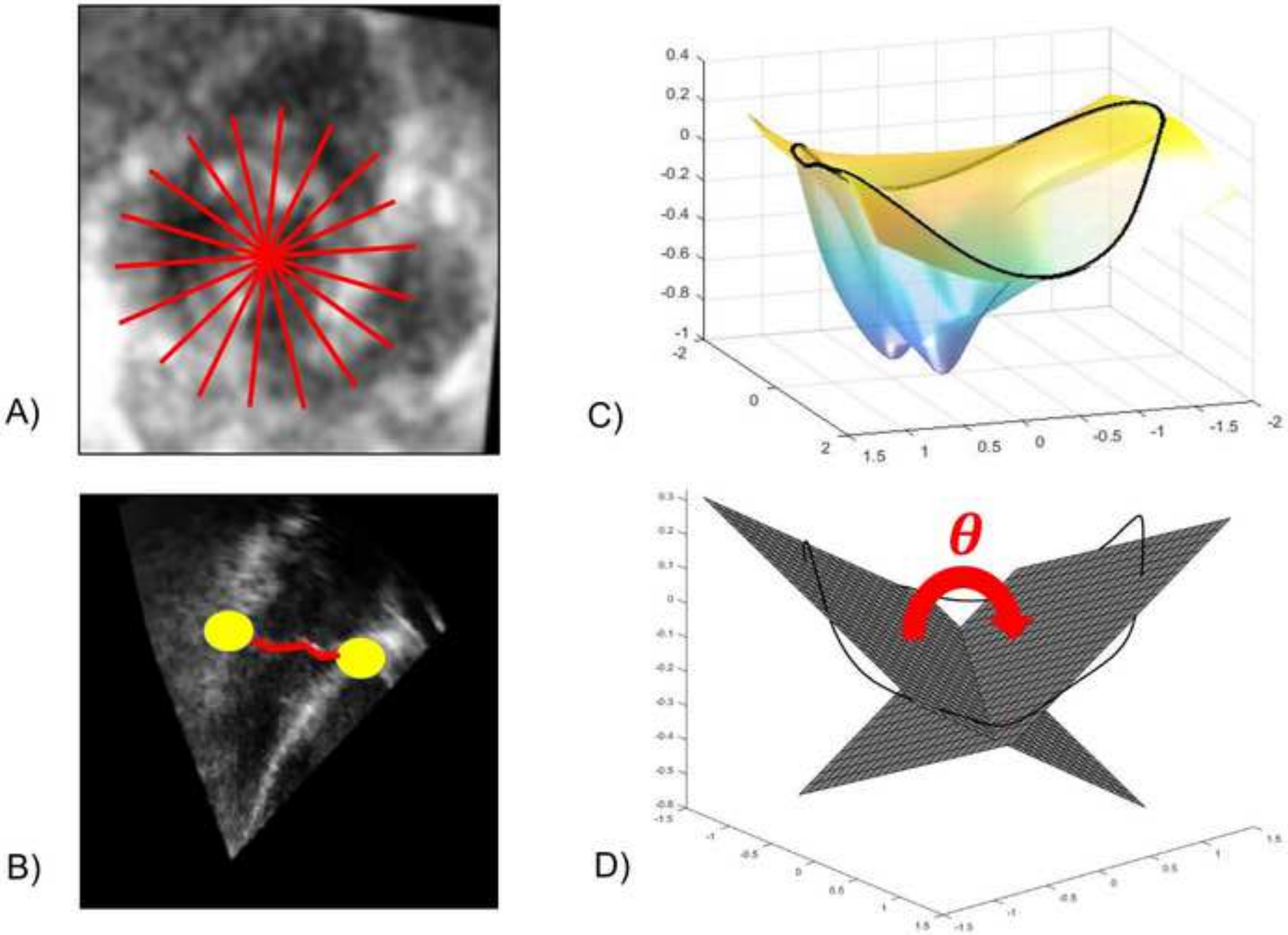

Tricuspid valves with annulus opened with a cut through the posteroseptal commissure and placed on the imaging stage in a

Click here to access/download;Figure;Figure 6.jpg

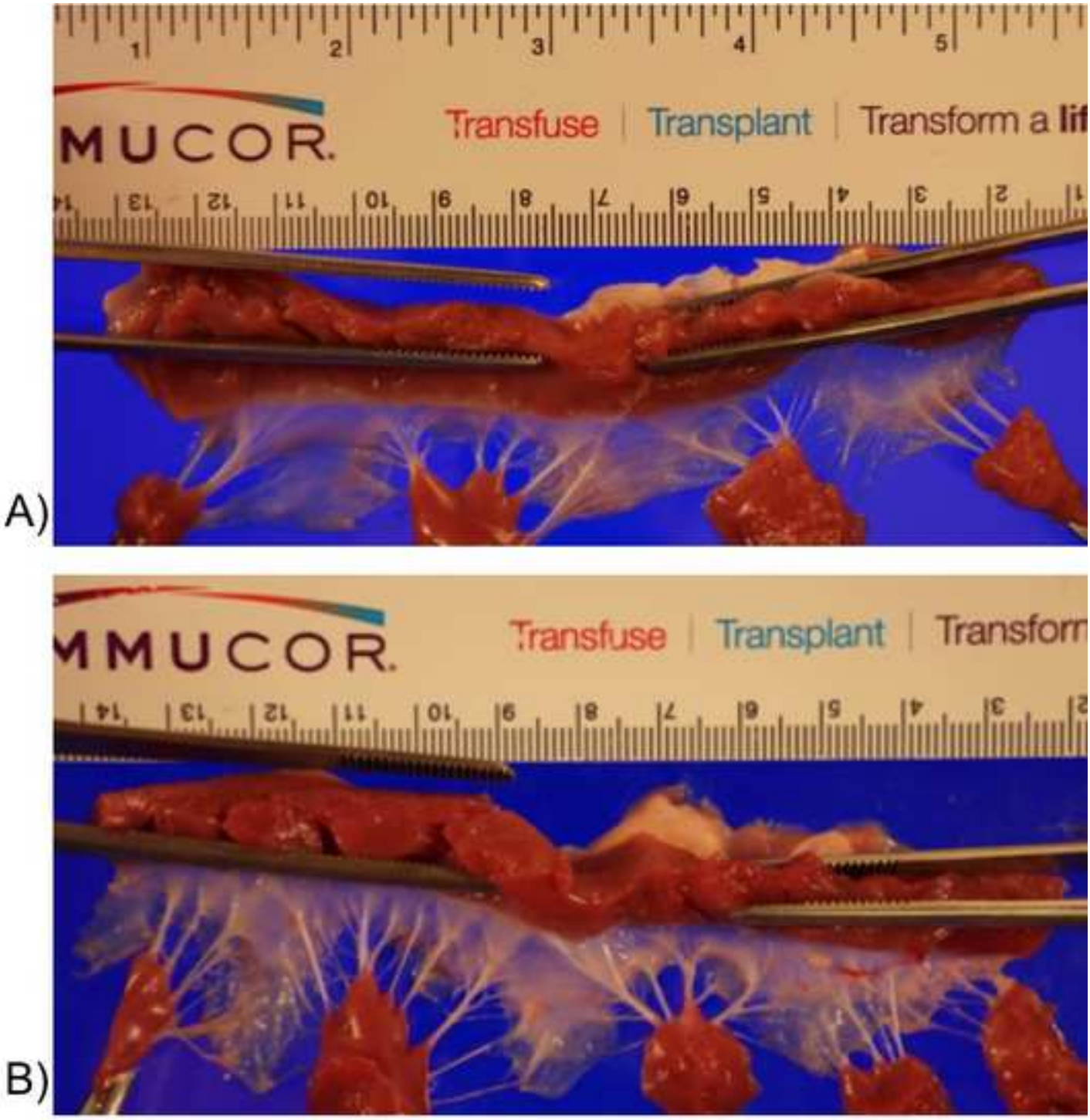

Comparisons of hemodynamic, echocardiographic pathologic parameters between intervention and control piglet groups for

Click here to access/download;Table;Table 1.xlsx

Table 1. Comparisons of hemodynamic, echocardiographic pathologic paramet

Parameters	Control Piglets
Weight at euthanasia (kg)	33.8 (28.1, 36.3)
RV systolic pressure/arterial systolic pressure (%)	30.0 (28.8, 33.3)
Pulmonary regurgitation grade (0-4)	1.0 (1.0, 1.0)
Tricuspid regurgitation grade (0-4)	2.0 (1.4, 2.0)
RV wall thickness (mm)	4.3 (4.0, 5.1)
Anterior papillary muscle cross-sectional area (cm^2)	0.4 (0.3, 0.5)
RV end diastolic area (cm^2)	10.8 (7.9, 12.1)
RV Fractional Area Change (%)	49.3 (47.7, 55.9)

NS denotes non-significance.

ters between intervention and control piglet groups for model validation. Data valu

Intervention Piglets	P-value
31.7 (27.7, 37.5)	NS
78.0 (64.8, 82.5)	<0.001
4.0 (3.4, 4.0)	<0.001
3.0 (2.0, 3.6)	0.02
9.3 (8.9, 11.0)	<0.001
1.1 (0.9, 1.5)	<0.001
20.3 (16.2, 23.8)	0.004
32.5 (26.1, 40.5)	<0.001

ues are expressed as median (25th, 75th percentile) with Mann-Whitney U test p-va

ılues reported.

Comparisons of tricuspid valve 3D echocardiographic parameters between intervention and control piglet groups. Values expressed

Click here to access/download;Table;Table 2.xlsx

Table 2. Comparisons of tricuspid valve 3D echocardiographic parameters betv

Parameters	Control Piglets (N=4)
TV annular circumference (cm)	8.6 (7.6, 9.3)
TV annulus lateral width dimension (cm)	2.5 (2.0, 2.7)
TV annulus anteroposterior dimension (cm)	3.1 (2.7, 3.3)
TV annulus width/anteroposterior dimension ratio	0.8 (0.7, 0.9)
TV annulus bending angle (degrees)	154 (145, 158)
TV Leaflet Area (cm2) at mid-systole	3.0 (2.7, 3.1)

ween intervention and control piglet groups. Values expressed as median (25th, 75th

Intervention Piglets (N=4)	P-value
11.4 (10.8, 12.0)	0.03
3.8 (3.4, 4.5)	0.02
3.5 (3.3, 3.8)	0.06
1.1 (1.0, 1.2)	0.02
150 (141, 158)	0.9
5.1 (4.1, 5.5)	0.03

ղ percentile) with Mann-Whitney test p-values reported.

Table of Materials

Click here to access/download;Table of Materials;Piglet TV Model Materials.xlsx

Name of Material/Equipment	Company/Supplier	Catalog Number	Comments/Description
Drugs			
1% lidocaine spray	WDDC	103365	Lidodan 30 mL
atropine sodium injection	WDDC/Rafter 8 Products		0.5 mg/mL
bupivacaine	WDDC/Sterimax		5 mg/mL
buprenorphine HCl slow release injection	Chiron Compounding Pharmacy		1 mg/mL
buprenorphine regular	WDDC/Champion Alstoe	121378	Vetergesic 0.3 mg/mL
cefazolin	WDDC/Fresenius Kabi	102016	1 g/vial
cephalexin capsule	WDDC/Novopharm		Novo-Lexin 250 mg/capsule
epinephrine	WDDC		Adrenalin (1:1000) 1 mg/mL
furosemide tablet	WDDC/Novopharm		10 mg tablet
Iodine Scrub/Spray	Cardinal Health	KF22422	Betadine brand
ketamine hydrochloride injection	WDDC/Vetoquinol	131771	Narketan 100 mg/mL
midazolam	WDDC/Sandoz	101100	5 mg/mL
norepinephrine	WDDC		1 mg/mL
pentobarbital sodium	WDDC/Bimeda-MTC	127189	Euthanyl 240 mg/mL
ranitidine injection	WDDC		25 mg/mL
ranitidine tablet	Sanis		300 mg tablet
Surgical Scrub Sponge	Stevens	333-377479	4% CHG Surgical Soap scrub brush
Equipment			
24G peripehral IV catheter	BD		Insyte-N
5Fr double lumen central venous catheter	Arrow	CS-14502	20cm
5Fr single lumen umbilical vessel catheters	Covidien/Kendall	8888160333	Argyle 15 inches
6" Chest retractor	RRSMRI		
6Fr triple lumen central venous catheter	Arrow	JR-42063-HPHNM	20cm

7Fr catheter sheath with flange	Dr. Coe custom designed		
Adson forceps	RRSMRI		
Aestiva/5 Ventilator	GE Datex Ohmeda		
Atraumatic forceps	Teleflex	351865	
bioptome	Dr. Coe lab		Mansfield Biopsy Forceps
Curved hemostat	RRSMRI		
Curved mosquito hemostat	RRSMRI		
Debakey Forceps (Long)	Teleflex	351804	
Debakey Forceps (Narrow)	Teleflex	351802	
Debakey Forceps (Rg)	Teleflex	351800	
Echo probe cover	Civco		
Endotracheotube	Stevens	180-112082055	Rusch Murphy Eye Low Press. Cuff
Iris Spring scissors	Fisher Scientific	NC0127560	
iSTAT 1 blood gas analyzer	Abbott Laboratories		MN:300-G
iSTAT CG4+ cartridges	Abbott Laboratories	03P85-50	
Kelly Hemostat	Fine Science Tools	1301914	
Kocher forceps	RRSMRI		
Large Army/Navy Retractor	RRSMRI		
Laryngoscope	MACO CE Miller#4 Blade	LA6226-4	Macolaryngoscope.com
Liga-clip applicator L	Ethicon	LC430	
Liga-clip applicator M	Ethicon	LX210	
Liga-clip applicator S	Ethicon	LX110	
Metal suction tip	RRSMRI		
Metzenbaum Scissors (Lg)	RRSMRI		
Metzenbaum Scissors (Md)	RRSMRI		
Mixter - long/mid wide	RRSMRI		
Mixter - long/narrow	RRSMRI		
Mixter - long/wide	RRSMRI		
Mixter - short/narrow	RRSMRI		
Needle Driver 10"	RRSMRI		

Needle Driver 6"	RRSMRI		
Needle Driver 7"	RRSMRI		
Philips iE33 Echocardiography machine	Philips		X7 and S12 probes
pressure line tubing and 3-way stopcock	Dr. Freed lab		
Rat tooth forcep	RRSMRI		
silastic reinforced sheeting	Bioplexus	SH-21001-040	6" x 8" x .040" Gloss
Small Army/Navy Retractor	RRSMRI		
Straight hemostat	RRSMRI		
Straight mosquito hemostat	RRSMRI		
Sutures: 4-0 and 5-0 synthetic, non-absorbable suture, 2-0 silk	Dr. Freed lab		
Towel clamp	RRSMRI		
vascular tourniquet	Dr. Freed lab		
Weitlaner retractor (Md)	RRSMRI		
Weitlaner retractor (Sm)	RRSMRI		
Zoll R Series Monitor Defibrillator	Zoll technologies		

Rebuttal Letter
Click here to access/download;Rebuttal Letter;Letter to Editor JOVE third revision June 3.docx

Dr. Nam Nguyen
Manager of Review
Journal of Visualized Experiments

Ref.: submission JoVE61251
A novel right ventricular volume and pressure loaded piglet heart model for the study of tricuspid valve function

June 3, 2020

Dear Dr. Nguyen,

Thank you for this opportunity to further readdress the reviewer comments and resubmit the above-named manuscript to the *Journal of Visualized Experiments*.

In this latest revision, we have included representative data that outlines some changes to the tricuspid valve due to our model. We hope these additional revisions are satisfactory and look forward to your review and reply.

Yours sincerely,

Lily Lin, MD, FRCPC (corresponding author)
Pediatric Cardiology
Stollery Children's Hospital
University of Alberta, Edmonton, Canada
Email: lily.lin@ualberta.ca